Journal of Chromatography A, 1232 (2012) 128–133

Contents lists available at SciVerse ScienceDirect

Journal of Chromatography A

journal homepage: www.elsevier.com/locate/chroma

Stereochemical characterization of fluorinated 2-(phenanthren-1-yl)propionic acids by enantioselective high performance liquid chromatography analysis and electronic circular dichroism detection

Carlo Bertucci[a,*], Marco Pistolozzi[a], Daniele Tedesco[a], Riccardo Zanasi[b], Renzo Ruzziconi[c], Anna Maria Di Pietra[a]

[a] Department of Pharmaceutical Sciences, University of Bologna, Italy
[b] Department of Chemistry and Biology, University of Salerno, Italy
[c] Department of Chemistry, University of Perugia, Italy

ARTICLE INFO

Article history:
Available online 9 November 2011

Keywords:
Enantioselective HPLC
Circular dichroism detection
Absolute configuration
Enantiomeric excess

ABSTRACT

Enantioselective high performance liquid chromatography (HPLC) coupled with a detection system based on the simultaneous measurement of UV absorption and electronic circular dichroism (ECD) allows a complete stereochemical characterization of chiral compounds, once the relationship between sign of the chiroptical properties and absolute configuration is determined. In the present communication, the development of enantioselective HPLC methods for the resolution of a series of fluorinated 2-phenanthrenylpropionic acids (**1**–**6**) is reported. Different chiral stationary phases (CSPs) were tested: Chiralcel® OJ, Chiralcel® OD, Chiralpak® AD, (*S*,*S*)-Whelk-O® 1, Chirobiotic™ T and α_1-acid glycoprotein (AGP). The results allow the application of the methods to a reliable determination of the enantiomeric excess for all the examined compounds; the highest enantioselectivity values were obtained with the Hibar® [(*S*,*S*)-Whelk-O® 1] column for some of the examined compounds. In the case of *rac*-2-(6-fluorophenanthren-1-yl)propionic acid (**1**), the relationship between circular dichroism and absolute configuration of the enantiomeric fractions was determined by ECD analysis and time-dependent density functional theory (TD-DFT) calculations. The experimental ECD spectrum of the second-eluted fraction of **1** on the Hibar® [(*S*,*S*)-Whelk-O® 1] column was found to be in excellent agreement with the theoretical ECD spectrum of (*S*)-**1**; therefore, the absolute configuration of the first- and second-eluted enantiomers on the (*S*,*S*)-Whelk-O® 1 CSP was assessed as (*R*) and (*S*), respectively, and the elution orders of the enantiomeric forms of **1** were determined on all the different CSPs.

1. Introduction

Fluorinated profens have received particular consideration in reference to their biological activity as successful non-steroidal anti-inflammatory drugs (NSAIDs), especially in connection with the presence of fluorine in the molecule. In fact, once placed in a specific position of a bioactive molecule, fluorine can substantially affect its chemical stability [1–6], thus slackening the related metabolic processes. Moreover, since the C–F bond is stronger than the C–H bond and exhibits reverse polarity, replacement of the α-hydrogen with the quasi-isosteric fluorine conveys a higher configurational stability to the chiral center of profens [7], thus allowing the drug pharmacodynamics, as well as the stereochemical matching with the biological target, to be investigated.

Since the biological activity of 2-(phenanthren-1-yl)propionic acid as a NSAID was reported to be similar to that of fenbufen [8], a number of nucleus and/or side-chain fluorinated 2-phenantrylpropionic acids were prepared [9], in order to assess the effect of fluorine on the structure/activity relationship with respect to its position and to the configuration of the chiral carbon. Nevertheless, a reliable study on the relationship between stereochemistry and biological activity requires a full stereochemical characterization of the compounds under investigation.

In this article, the development of enantioselective high performance liquid chromatography (HPLC) methods for the resolution of a series of 2-(fluorophenanthren-1-yl)propionic acids (**1**–**6**, Fig. 1) is reported; these methods may be applied for the determination of the enantiomeric excess (e.e.). For one of these compounds, 2-(6-fluorophenanthren-1-yl)-propionic acid (**1**), the enantioselective method has been scaled up to allow the collection of the enantiomeric fractions, before their stereochemical characterization. The e.e. value was determined through the same chromatographic

* Corresponding author. Tel.: +39 051 2099 731; fax: +39 051 2099 734.
E-mail address: carlo.bertucci@unibo.it (C. Bertucci).

0021-9673/$ – see front matter © 2011 Elsevier B.V. All rights reserved.
doi:10.1016/j.chroma.2011.10.090

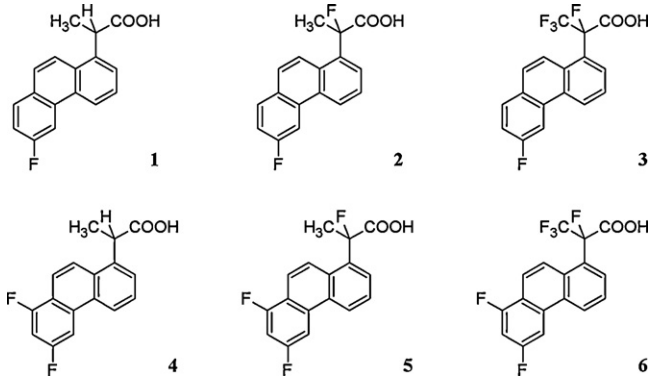

Fig. 1. 2-(Fluorophenanthren-1-yl)propionic acids.

assay, and the absolute configuration was assessed by electronic circular dichroism (ECD) spectroscopy and time-dependent density functional theory (TD-DFT) computations.

2. Experimental

2.1. Materials

Compounds **1**–**6** were prepared as previously reported [9]. *n*-Hexane, acetonitrile, methanol, ethanol, 1-propanol, 2-propanol, glacial acetic acid, formic acid, triethanolamine and triethylamine were purchased from Sigma–Aldrich (Milan, Italy). All solvents used to prepare solutions and mobile phases were HPLC or analytical grade. K_2HPO_4 and KH_2PO_4 powders were purchased from Carlo Erba Reagenti (Milan, Italy). Water was doubly distilled and buffers were filtered through a 0.22 μm membrane filter.

2.2. HPLC analysis

2.2.1. Instrumentation

A Varian (Palo Alto, CA, USA) Mod. 5000 HPLC system with a HP 1040A diode array detector (Hewlett Packard, Waldbronn, Germany) was used for the development of enantioselective methods and the collection of enantiomeric fractions. The e.e. determination with simultaneous monitoring of UV and ECD signals of compound **1** were carried out using a Jasco (Tokyo, Japan) HPLC system consisting of a Jasco PU-980 pump, a Jasco MD 910 multiwavelength detector and a CD-995 chiral detector, equipped with a 25 mm pathlength HPLC flow cell. Samples were injected by a 20 μL loop in both instruments.

The following HPLC columns were used, having different chiral stationary phases (CSPs): Chiralcel® OJ (250 × 4.6 mm I.D., 10 μm) and Chiralpak® AD (250 × 4.6 mm I.D., 10 μm), purchased from Daicel, Chiral Technologies Europe, Illkirch, France; Chiralcel® OD (250 × 4.6 mm I.D., 10 μm; Daicel, Millinckrodt Baker B.V., Deventer, Holland); Hibar® pre-packed column RT (250 × 4.6 mm I.D., 5 μm, customized packing (*S*,*S*)-Whelk-O® 1; Merck KGaA, Darmstadt, Germany); Chirobiotic™ T (250 × 4.6 mm I.D., 5 μm; Astec, Whippany, NJ, USA), and Chiral-AGP (100 × 4.0 mm I.D., 5 μm; ChromTech AB, Sollentuna, Sweden).

2.2.2. Chromatographic conditions

Stock solutions of compounds **1**–**6** (1.0 mg mL^{-1}) in 2-propanol and in methanol were prepared for direct-phase and reversed-phase chromatography, respectively. Stock solutions were further diluted in the same solvents to a concentration range between 0.02 and 0.1 mg mL^{-1}.

Mobile phases used in direct-phase chromatography were prepared with hexane and 2-propanol, adding formic acid or acetic acid to improve the chromatographic resolution. In particular, hexane/2-propanol/acetic acid mobile phases were used with Chiralcel® OJ (79:20:1; 79.5:20:0.5; 69:30:1; 89.5:10:0.5; 80:20:0, v/v/v), and Hibar® [(*S*,*S*)-Whelk-O® 1] columns (80:20:0; 79.5:20:0.5; 90:10:0; 89.5:10:0.5; 94.5:5:0.5, v/v/v), while hexane/2-propanol/formic acid mobile phases were used with Chiralcel® OD (69.5:30:0.5; 79.5:20:0.5; 89.5:10:0.5, v/v/v) and Chiralpak® AD (70:30:0; 69.5:30:0.5, v/v/v) columns.

The Chiralcel® OD column was also successfully used to separate and collect the single enantiomers of compound **1** (mobile phase, 79:5:20:0.5, v/v/v hexane/2-propanol/formic acid; flow 1 mL min^{-1}, λ: 250 nm). The e.e. of each fraction of **1** was determined by using the (*S*,*S*)-Whelk-O® 1 CSP (mobile phase, 79.5:20:0.5 v/v/v hexane/2-propanol/acetic acid; flow 1 mL min^{-1}, λ: 295 nm). The enantiomeric fractions were dried under nitrogen, reconstituted with 2-propanol and analyzed by UV spectroscopy to determine their concentration.

In reversed-phase chromatography, solutions of triethylamine (TEA) acetate buffer at different pH values mixed with methanol or acetonitrile and phosphate buffer/1-propanol (PB) were used with Chirobiotic™ and Chiral-AGP columns, respectively.

Triethylamine (TEA) acetate buffer was prepared adding acetic acid to aqueous triethylamine to adjust the pH value. The following mobile phases were used: TEA acetate (20 mM, pH 5, 6 and 7)/methanol 90:10, v/v; TEA acetate (20 mM, pH 6)/methanol (75:25; 80:20; 95:5, v/v); TEA acetate (20 mM, pH 6)/acetonitrile (80:20; 90:10; 95:5, v/v). Replacement of triethylamine by triethanolamine did not show any significant difference. Phosphate buffer (PB, 0.1 M, pH 6) was obtained by adding a 0.1 M aq. KH_2PO_4 (pH ∼ 4) to 0.1 M aq. K_2HPO_4 (pH ∼ 9). Mobile phases consisted in PB/1-propanol mixtures (90:10; 95:5, v/v). All mobile phases were degassed by sonication. Flow rate was maintained between 0.6 and 1.5 mL min^{-1}.

The enantioselectivity (α) was calculated as $\alpha = k'_2/k'_1$, where k'_2 and k'_1 are the capacity factors of the second- and first-eluted enantiomers, respectively. Capacity factors (k') are defined as $k' = t_r - t_0/t_0$, where t_r is the retention time of the analyte, and t_0 is the retention time of a non-retained solute. The enantiomeric excess was determined as e.e. = ([A] − [B])/([A] + [B]) × 100, where [A] and [B] are the peak areas of the most and less abundant enantiomers, respectively.

2.3. UV and ECD measurements

UV spectra of compounds **1**–**6** were carried out on a spectrophotometer Jasco V-520, in 2-propanol at room temperature, using 1 cm pathlength cells.

ECD spectra (370–210 nm spectral range) of the single enantiomeric fractions of **1** were recorded on a Jasco J-810 spectropolarimeter, in 2-propanol at room temperature, using a 1 cm pathlength cell. Concentrations were adjusted to keep the absorbance in the optimum photometric range. Spectra were recorded at 0.5 nm intervals using a 2 nm spectral bandwidth, a 20 nm min^{-1} scan rate and a 4 s time constant. The actual concentration of the fractions of **1** was determined by UV analysis.

2.4. Conformational analysis and ECD calculation

Molecular mechanics (MM) calculations were carried out for a preliminary conformational analysis of (*S*)-**1** (Fig. 2). The conformer distribution was determined at the MMFF94s [10] level using the Spartan'02 software [11], and the relative energies (ΔE_{MM}) with

Table 1
Resume of the best chromatographic conditions and parameters for the separation of racemic mixtures of compounds **1**–**6**.

Column	Compound	Mobile phase	t_0 (min)	k'_1	α
Chiralcel®OJ	1	Hexane/2-propanol/acetic acid 69:30:1, v/v/v	2.89	1.51	1.16
	2			1.97	1.74
Chiralcel®OJ	4	Hexane/2-propanol/acetic acid 79.5:20:0.5, v/v/v	2.89	1.08	1.32
Chiralcel®OD	1	Hexane/2-propanol/formic acid 69:30:1, v/v/v	3.23	0.60	1.30
Chiralpak®AD	2	Hexane/2-propanol/formic acid 69:30:1, v/v/v	3.49	1.37	1.23
Hibar® [(*S*,*S*)-Whelk-O® 1]	1	Hexane/2-propanol/acetic acid 79.5:20:0.5, v/v/v	2.80	1.45	2.15
	2			0.84	2.05
	4			0.93	2.07
	5			0.59	1.83
Chiral-AGP	1	PB (0.1 M, pH 6)/1-propanol 95:5, v/v	2.08	7.51	1.56
	2			5.69	1.79
	3			10.95	1.53
	4			8.54	1.19
	5			4.71	2.70
	6			14.51	2.44
Chirobiotic™ T	1	TEA acetate (20 mM, pH 6)/methanol 75:25, v/v	3.33	1.63	1.15

respect to the lowest-energy conformation were calculated for each conformer.

Full quantum mechanical (QM) geometry optimizations were then performed through density functional theory (DFT) [12,13] calculations on the MM conformers having $\Delta E_{MM} \leq 3$ kcal mol^{-1}, using the Gaussian 09 software package [14]. The hybrid B3LYP exchange-correlation functional [15–18] was used in combination with the triple-zeta, double-polarization TZ2P basis set; [19,20] solvent effects were accounted for 2-propanol by adopting the polarizable continuum model (PCM) in its integral equation formalism [21], as implemented within the Gaussian 09 package. The Boltzmann distribution of conformers at 298.15 K and 1 atm was calculated from relative self-consistent field energies (ΔE_{QM}), and relative free energies (ΔG).

Time-dependent DFT (TD-DFT) [22] calculations of the chiroptical properties of (*S*)-**1** were performed at the B3LYP/TZ2P level on the optimized geometries of conformers with $\Delta E_{QM} \leq 3$ kcal mol^{-1}; excitation wave numbers (σ_{mn}) and rotational strengths (R_{mn}) were determined for the lowest 50 excited states of each conformer. Theoretical ECD spectra as a function of wave number [$\Delta\varepsilon(\sigma)$] were derived for (*S*)-**1** by approximation of all R_{mn} values to Gaussian functions ($\Delta\sigma = 0.3$ eV), summation over all excited states and conformational averaging, according to the Boltzmann distribution of conformers [23,24].

Theoretical spectra were converted in wavelength scale for a convenient comparison with experimental data; the correlation between the theoretical ECD spectrum of (*S*)-**1** and the experimental ECD spectra of the enantiomeric fractions of **1** was then evaluated by the Pearson product-moment correlation coefficient (r) [25].

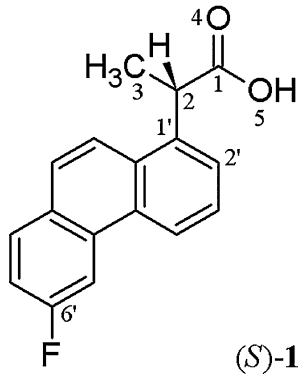

Fig. 2. (2*S*)-2-(6-Fluorophenanthren-1-yl)propionic acid [(*S*)-**1**].

3. Results and discussion

3.1. Enantioselective HPLC analysis

The development of enantioselective assays to determine the e.e. values for the series of 2-(fluorophenanthren-1-yl)propionic acids required the screening of several CSPs and various experimental conditions. Among the various direct-mode columns tested, Chiralcel® OJ proved to be efficient in the resolution of compounds **1**, **2** and **4** (Table 1, S.1). The mobile phases were prepared with hexane and 2-propanol, adding acetic acid to improve the efficiency of the separation process. The increase in 2-propanol concentration determined a significant decrease in retention times, while the enantioselectivity did not change significantly (Table S.1). Chiralcel® OD was successfully employed in the enantiomeric resolution of compounds **1** while Chiralpak® AD was effective in resolving compound **2** (Table 1, S.2 and S.3). Changes in both the nature of the mobile phase and the flow rate, did not allow the resolution of the other compounds of the series (Tables S.2 and S.3). The Hibar® [(*S*,*S*)-Whelk-O® 1] column was efficient for the enantiomeric resolution of most of the 2-(fluorophenanthren-1-yl)propionic acids under investigation (Table 1, S.4). As an example, the enantiomeric resolution of *rac*-**4** is shown in Fig. 3. Higher polarity of the mobile phase caused a significant reduction in retention times (Table S.4). This CSP resulted particularly efficient and suitable to determine the e.e. values of enriched fractions of these compounds.

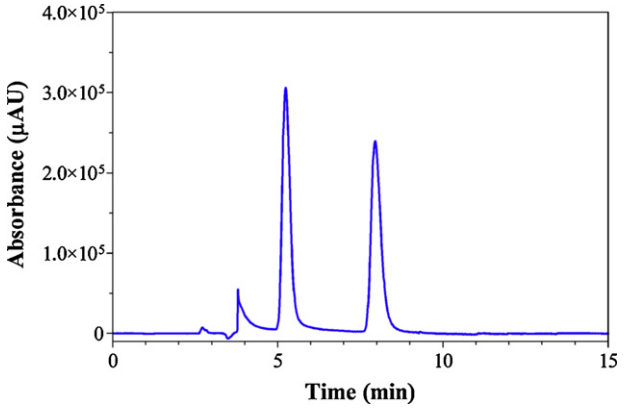

Fig. 3. Chromatogram relative to the enantioresolution of *rac*-**4**, 0.1 mg mL^{-1}, obtained on Hibar® [(*S*,*S*)-Whelk-O® 1] column. Mobile phase: *n*-hexane/2-propanol/acetic acid 79.5:20:0.5, v/v/v, flow 1 mL min^{-1}; UV detection (λ = 250 nm).

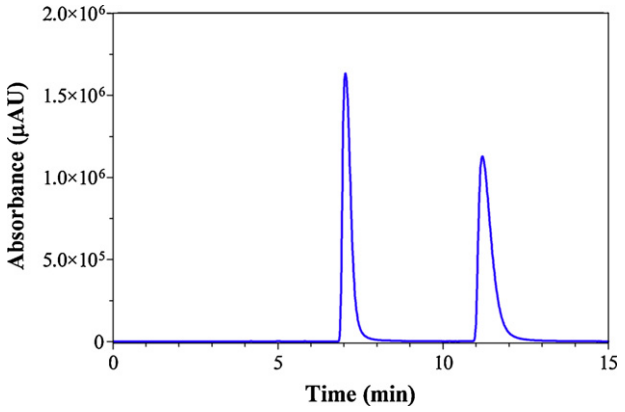

Fig. 4. Chromatogram relative to the enantioresolution of *rac*-**1**, 1 mg mL^{-1}, obtained on Hibar® [(*S*,*S*)-Whelk-O® 1] column. Mobile phase: *n*-hexane/2-propanol/acetic acid 79.5:20:0.5, v/v/v, flow 1 mL min^{-1}; UV detection (λ = 250 nm).

AGP proved to be a very efficient reversed-phase CSP in resolving all the examined compounds (Table 1, S.5), while Chirobiotic™ T was effective in the resolution of compound **1** (Table 1, S.6). In the case of AGP, the interaction of the analytes with the chiral selector was strongly affected by the concentration of the organic modifier in the mobile phase, as shown by the significant reduction in k' and α values as the 2-propanol content increases from 5 to 10% (Table S.5).

The elution of *rac*-**1** on the Hibar® [(*S*,*S*)-Whelk-O® 1] column was monitored by the simultaneous measurements of both absorption and ECD signals (Fig. 4) [26]. The chromatographic profiles obtained by monitoring the ECD signal showed a different sign of the two peaks, as a result of the enantiomeric ECD signals of the single enantiomers. The analysis performed on both Hibar® [(*S*,*S*)-Whelk-O® 1] and Chiral-AGP columns exhibited a reverse elution order of the enantiomers of **1** with respect to Chiralcel® OJ and Chiralcel® OD.

3.2. Absolute configuration assignment to the enantiomers of **1**

The enantiomeric fractions of **1** were obtained by preparative enantioselective HPLC on a Chiralcel® OD column. Repetitive injections and collection of the enantiomeric fractions yielded about 0.3 mg of each enantiomer. The e.e. resulted 97.3 and 97.4% for the first- and second-eluted fraction, respectively, as determined by the chromatographic assay developed on the Hibar® [(*S*,*S*)-Whelk-O® 1] column (Fig. 5). The experimental ECD spectra were carried out by analyzing the reconstituted solutions in 2-propanol. The UV absorption spectra, as well as the specular ECD spectra, (Fig. 6) show three structured bands, the lowest-energy one in the 350–320 nm spectral region, the second one in the 280–250 nm region, and the highest energy one centered at about 230 nm. The absolute configuration of the enantiomers of **1** was then determined by comparison of the experimental ECD spectra of the two fractions with the theoretical ECD spectrum calculated for (*S*)-**1** [23]. The latter was obtained by conformational averaging, taking into account the contributions of the lowest-energy conformations and their populations. The conformational flexibility of the propionic moiety may be conveniently described by two dihedral angles: ϕ_1 (C1–C2–C1′–C2′), describing the rotation about the C2–C1′ bond and to the mutual orientation of the propionic and fluorophenanthrenyl moieties and ϕ_2 (O4-C1–C2–C1′), describing the rotation about the C1–C2 bond and the orientation of the carboxyl group. The conformational analysis at the MM level led to the identification of seven conformers (**a**–**g**, Table 2) with $\Delta E_{MM} \leq 3$ kcal mol^{-1}. DFT geometry optimization caused some MM conformers to converge to the same geometry: conformational clustering was carried out with a threshold RMSD value of 0.01 Å (Tables S.7 and S.8). As a result, four conformers (**h**–**k**, Table 3) were obtained by calculations without solvation models (gas phase), while six conformers (**l**–**q**, Table 4) were obtained by calculations with IEFPCM for 2-propanol. Graphical representations of the different conformers are reported in the supporting information (Figs. S.1 and S.2).

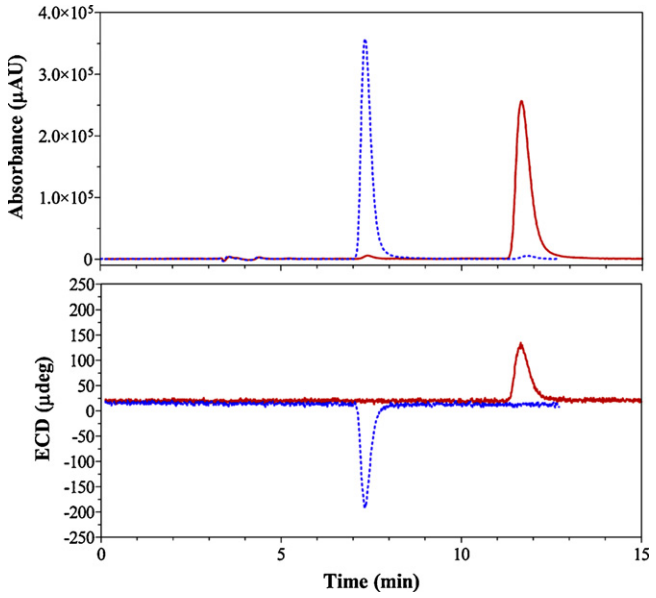

Fig. 5. Enantiomeric excess determination for the enantiomeric fractions of **1**. (Dashed) First-eluted fraction. (Solid) Second-eluted fraction. 1 mg mL^{-1}, obtained on Hibar® [(*S*,*S*)-Whelk-O® 1] column. Mobile phase: *n*-hexane/2-propanol/acetic acid 79.5:20:0.5, v/v/v, flow 1 mL min^{-1}; simultaneous UV and ECD detection (λ = 295 nm).

The optimized conformers showed different theoretical ECD profiles (Figs. S.3 and S.4; rotational strengths and excitation energies in the 340–200 nm range are reported in Tables S.9 and S.10); this behavior is consistent with the different orientations of the phenanthryl chromophore with respect to the propionic

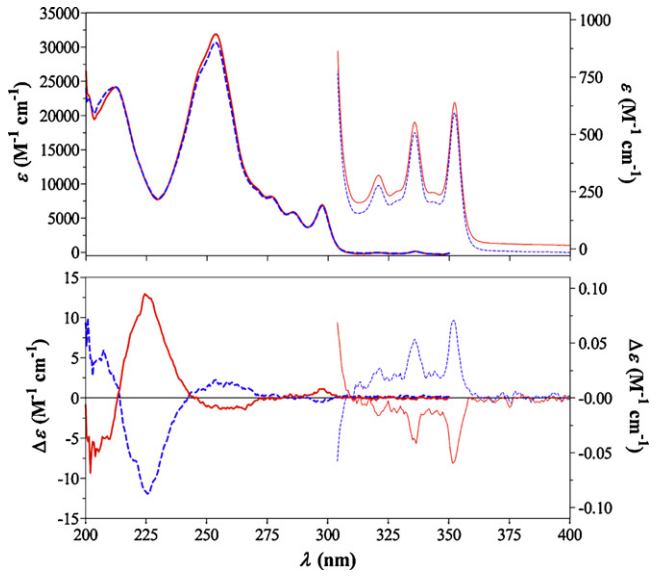

Fig. 6. UV and ECD spectra for the enantiomeric fractions of **1** in 2-propanol (pathlength: 1 cm). (Dashed) First-eluted fraction (400–300 nm: 711 μM; 350–200 nm: 17.8 μM). (Solid) Second-eluted fraction (400–300 nm: 646 μM; 350–200 nm: 16.2 μM). Elution order determined on Hibar® [(*S*,*S*)-Whelk-O® 1] column.

Table 2
Geometrical parameters, energy values and fractional equilibrium populations for the conformers of (*S*)-**1**, as obtained after MM conformational analysis.

Conformer	ϕ_1 (deg)	ϕ_2 (deg)	E_{MM} (kcal mol^{-1})	ΔE_{MM} (kcal mol^{-1})	χ_{MM}[a]
1a	−96.543	57.372	49.432	0.000	0.3064
1b	123.030	121.692	49.503	0.071	0.2718
1c	−45.365	99.875	49.824	0.392	0.1581
1d	−101.334	−114.372	49.868	0.436	0.1468
1e	121.244	−40.141	50.395	0.963	0.0603
1f	−46.781	−11.567	50.455	1.023	0.0545
1g	125.385	141.077	52.379	2.947	0.0021

[a] Calculated using Boltzmann statistics at 298.15 K.

Table 3
Geometrical parameters, energy values and fractional equilibrium populations for the conformers of (*S*)-**1**, as obtained after DFT geometry optimization (B3LYP/TZ2P) in gas phase.

Conformer	ϕ_1 (deg)	ϕ_2 (deg)	E_{QM} (Hartree/particle)	ΔE_{QM} (kcal mol^{-1})	χ_{QM}[a]	G (Hartree/particle)	ΔG (kcal mol^{-1})	χ_G[a]
1h	−41.419	−81.720	−906.29110978	0.000	0.5304	−906.078785	0.000	0.7250
1i	122.935	130.731	−906.29042587	0.429	0.2570	−906.077137	1.034	0.1265
1j	−104.315	−119.335	−906.29017972	0.584	0.1981	−906.077240	0.970	0.1411
1k	120.133	−43.138	−906.28771135	2.133	0.0145	−906.074447	2.722	0.0073

[a] Calculated using Boltzmann statistics at 298.15 K.

Table 4
Geometrical parameters, energy values and fractional equilibrium populations for the conformers of (*S*)-**1**, as obtained after DFT geometry optimization (B3LYP/TZ2P) in 2-propanol (IEFPCM solvation model).

Conformer	ϕ_1 (deg)	ϕ_2 (deg)	E_{QM} (Hartree/particle)	ΔE_{QM} (kcal mol^{-1})	χ_{QM}[a]	G (Hartree/particle)	ΔG (kcal mol^{-1})	χ_G[a]
1l	−41.796	106.466	−906.30098721	0.000	0.4037	−906.088983	0.000	0.6203
1m	122.927	135.824	−906.30034049	0.406	0.2035	−906.087263	1.079	0.1003
1n	−104.913	37.596	−906.30030519	0.428	0.1960	−906.087626	0.852	0.1474
1o	−105.572	−127.412	−906.29999385	0.623	0.1409	−906.087346	1.027	0.1095
1p	120.389	−37.949	−906.29879378	1.376	0.0395	−906.085608	2.118	0.0174
1q	121.161	142.346	−906.29795970	1.900	0.0163	−906.084450	2.844	0.0051

[a] Calculated using Boltzmann statistics at 298.15 K.

moiety. Conformationally averaged ECD spectra differ when Boltzmann populations are calculated from ΔE_{QM} or ΔG; a stronger contribution of the lowest-energy conformer is observed for ΔG-based calculations, leading to increased intensities of the short-wavelength ECD bands. Implementation of IEFPCM for long-range solvent effects in TD-DFT calculations caused minimal changes in the conformationally averaged ECD spectrum of (*S*)-**1** (Fig. S.5), mainly consisting in a slight shift towards shorter wavelengths.

The comparison between the theoretical ECD spectrum of (*S*)-**1** and the experimental spectra of the enantiomeric fractions of **1** (Fig. 7) on the (*S*,*S*)-Whelk-O® 1 CSP shows a positive correlation between theoretical and experimental data for the second-eluted fraction, and a negative correlation for the first-eluted fraction (Table S.11). Better r values are obtained when ΔE_{QM}-based Boltzmann populations are used for the conformational averaging of the theoretical ECD spectrum. Further improvement in correlation coefficients would be obtained by shifting the theoretical ECD spectrum of (*S*)-**1** towards shorter wavelengths, which is consistent with the tendency of TD-DFT calculations to underestimate transition energies [23]. On this basis, the first- and second-eluted fractions on the (*S*,*S*)-Whelk-O® 1 CSP are identified as the (*R*)- and (*S*)-enantiomers of **1**, respectively.

Once the relationship between ECD and absolute configuration was established, it was possible to determine the elution orders for compound **1** not only on the (*S*,*S*)-Whelk-O® 1 CSP, but also on the other CSPs employed in the present investigation. In particular, the absolute configuration (*S*) can be assigned to the first-eluted enantiomer of **1** on Chiralcel® OJ and Chiralcel® OD, and to the second-eluted enantiomer on Chiral-AGP.

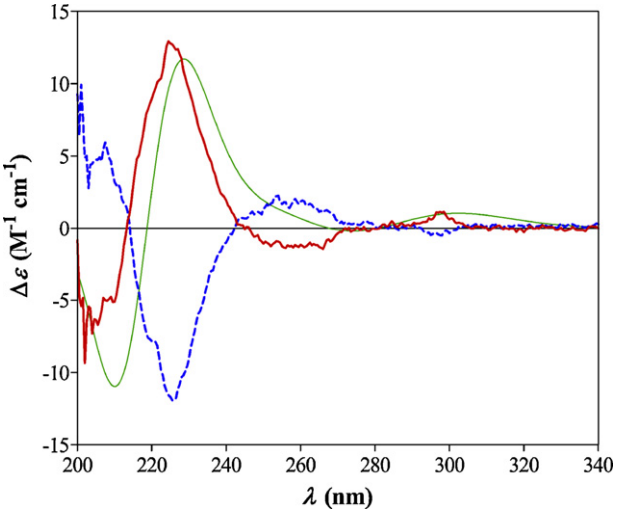

Fig. 7. Theoretical ECD spectrum for (*S*)-**1** and comparison with experimental data. (Thin) Theoretical ECD spectrum in 2-propanol (IEFPCM solvation model, ΔE_{QM}-based conformational averaging, $\Delta\sigma = 0.3$ eV). (Dashed) First-eluted enantiomeric fraction of **1**. (Solid) Second-eluted enantiomeric fraction of **1**. Elution order determined on Hibar® [(*S*,*S*)-Whelk-O® 1] column.

4. Conclusions

The developed enantioselective HPLC methods resulted efficient for the resolution of all the racemic mixtures under examination. Relatively high values of enantioselectivity were obtained on the Hibar® [(*S*,*S*)-Whelk-O® 1] and Chiral-AGP columns. The method was successfully scaled-up on the Chiralcel® OD column,

allowing to collect the enantiomeric fractions of **1** with high values of enantiomeric excess. Full stereochemical characterization of **1** was carried out by a combination of experimental ECD spectroscopy and theoretical TD-DFT calculations, which allowed to assign (*R*) and (*S*) absolute configuration to the first- and second-eluted enantiomers of **1** on the (*S*,*S*)-Whelk-O® 1 CSP, respectively. The elution order on the different CSPs was determined according to the detected ECD sign at 295 nm, which is negative for the (*R*)-enantiomer and positive for the (*S*)-enantiomer. This multi-technique approach proves to be very promising and may be applied for the stereochemical characterization of several compounds of biological and pharmaceutical interest.

Acknowledgements

The authors are grateful for financial support from the Universities of Bologna, Salerno and Perugia and from MIUR, Italy (PRIN 2008 National Program).

Appendix A. Supplementary data

Supplementary data associated with this article can be found, in the online version, at doi:10.1016/j.chroma.2011.10.090.

References

[1] M. Schlosser, in: V.A. Soloshonok (Ed.), Enantiocontrolled Synthesis of Fluoro-Organic Compounds: Stereochemical Challenges and Biomedical Targets, Wiley, Chichester, 1999.
[2] M. Schlosser, Angew. Chem. Int. Ed. 37 (1998) 1496.
[3] M. Schlosser, D. Michel, Tetrahedron 52 (1996) 99.
[4] M. Schlosser, Tetrahedron 34 (1978) 3.
[5] T. Welch, S. Eswarakrishnan, Fluorine in Bioorganic Chemistry, Wiley, New York, 1991.
[6] R. Filler, Y. Kobayashi (Eds.), Biomedical Aspects of Fluorine Chemistry, Kodansha/Elsevier Biomedical, Tokyo/Amsterdam, 1982.
[7] S.J. Hamman, Fluorine Chem. 60 (1993) 225.
[8] A. Eirín, F. Fernández, G. Gómez, C. López, A. Santos, J.M. Calleja, D. de la Iglesia, E. Cano, Arch. Pharm. (Weinheim) 320 (1987) 1110.
[9] G. Ricci, R. Ruzziconi, J. Org. Chem. 70 (2005) 611.
[10] T.A. Halgren, J. Comput. Chem. 20 (1999) 720.
[11] Spartan'02, Wavefunction, Inc., Irvine, CA, USA.
[12] P. Hohenberg, W. Kohn, Phys. Rev. 136 (1964) B864.
[13] W. Kohn, L.J. Sham, Phys. Rev. 140 (1965) A1133.
[14] M.J. Frisch, G.W. Trucks, H.B. Schlegel, G.E. Scuseria, M.A. Robb, J.R. Cheeseman, G. Scalmani, V. Barone, B. Mennucci, G.A. Petersson, H. Nakatsuji, M. Caricato, X. Li, H.P. Hratchian, A.F. Izmaylov, J. Bloino, G. Zheng, J.L. Sonnenberg, M. Hada, M. Ehara, K. Toyota, R. Fukuda, J. Hasegawa, M. Ishida, T. Nakajima, Y. Honda, O. Kitao, H. Nakai, T. Vreven, J.A. Montgomery, Jr., J.E. Peralta, F. Ogliaro, M. Bearpark, J.J. Heyd, E. Brothers, K.N. Kudin, V.N. Staroverov, R. Kobayashi, J. Normand, K. Raghavachari, A. Rendell, J.C. Burant, S.S. Iyengar, J. Tomasi, M. Cossi, N. Rega, J.M. Millam, M. Klene, J.E. Knox, J.B. Cross, V. Bakken, C. Adamo, J. Jaramillo, R. Gomperts, R.E. Stratmann, O. Yazyev, A.J. Austin, R. Cammi, C. Pomelli, J.W. Ochterski, R.L. Martin, K. Morokuma, V.G. Zakrzewski, G.A. Voth, P. Salvador, J.J. Dannenberg, S. Dapprich, A.D. Daniels, O. Farkas, J.B. Foresman, J.V. Ortiz, J. Cioslowski, D.J. Fox, Gaussian 09, Revision A.02, Gaussian, Inc., Wallingford, CT, 2009.
[15] A.D. Becke, J. Chem. Phys. 98 (1993) 5648.
[16] C. Lee, W. Yang, R.G. Parr, Phys. Rev. 37 (1988) B785.
[17] S.H. Vosko, L. Wilk, M. Nusair, Can. J. Phys. 58 (1980) 1200.
[18] P.J. Stephens, F.J. Devlin, C.F. Chabalowski, M.J. Frisch, J. Phys. Chem. 98 (1994) 11623.
[19] S. Huzinaga, J. Chem. Phys. 42 (1965) 1293.
[20] T.H. Dunning, J. Chem. Phys. 55 (1971) 716.
[21] J. Tomasi, B. Mennucci, R. Cammi, Chem. Rev. 105 (2005) 2999.
[22] R. Bauernschmitt, R. Ahlrichs, Chem. Phys. Lett. 256 (1996) 454.
[23] J. Autschbach, Chirality 21 (2009) E116.
[24] P.J. Stephens, N. Harada, Chirality 22 (2010) 229.
[25] J.R. Taylor, Introduction to Error Analysis, 2nd ed., University Science Books, Sausalito, CA, USA, 1997.
[26] P. Salvadori, C. Bertucci, C. Rosini, in: K. Nakanishi, N. Berova, R.W. Woody (Eds.), Circular Dichroism: Principles and Applications, VCH Publishers, New York, 1994, p. 541.